Id. EN-04

NEUTRONIC AND THERMAL HIDRAULIC STUDY OF ANNULAR PWR FUEL ASSEMBLIES USING UO_2 AND UN

Raphael H. M. Silva[1], Cristian G. Oliveira[1], Patrícia A. L. Reis[1], Maria A. F. Veloso[1], Clarysson A. M. Silva[1]

[1]Departamento de Engenharia Nuclear, UFMG, Departamento de Engenharia Nuclear (Universidade Federal de Minas Gerais, Av. Antônio Carlos, 6627, Campus UFMG, PCA 1, Bloco 04, Anexo Engenharia, Pampulha, 31270-90 Belo Horizonte, MG, Brazil)
raphagalo@eng-nucl.mest.ufmg.br; patricialire@yahoo.com.br; clarysson@nuclear.ufmg.br

Key words: PWR; Advanced Fuels; UN; Annular Fuel Assembly; SCALE6.0/NEWT; STHIRP

ABSTRACT

The conventional solid fuel UO_2 has been utilized in Light Water Reactors (LWR) over the past few years. It exhibits high temperatures in the central fuel zone and lower thermal conductivity compared to advanced proposed fuels. These features limit reactor power due to structural issues in the fuel rods, such as swelling, deformation, and the cracks formation. Thus, new fuel designs have been under study to enable enhanced thermal and mechanical efficiency, as well as increased reactor cycle length. In this sense, distinct fuel designs have been proposed, such as the annular geometry that implements a central cooling channel in the fuel rods aiming to provide temperature decreases in central fuel zone. Furthermore, a variety of fuel alloys have been evaluated, notably Uranium Mononitride (UN), mainly due to its superior thermal conductivity compared to UO_2. In this context, the present work studies the use of UO_2 and UN in annular fuel pin geometry for a typical Pressurized Water Reactor (PWR). Neutronic and thermal-hydraulic analyses were performed using the respective SCALE 6.0/NEWT and STHIRP codes. Distinct geometries of annular fuel assemblies (AFAs) were simulated, where the relative power distribution calculated by NEWT was used as input data for the STHIRP code. These geometries were compared with conventional PWR fuel assembly. The goal is to verify the physical parameters of annular fuel assemblies with intent to determine which could be used in PWRs according to neutronic and thermal-hydraulic analyses. Comparing the evaluated fuels, the largest thermal conductivity of UN contributes to largest heat conduction in the pellet zone and to lowest fuel temperature. About annular geometry, it presents a low fuel centerline temperature and lower heat flux in comparison to a solid fuel pin. As a result, improvements to safety margins and higher core power densities might be achieved.

1. INTRODUCTION

In recent years, there have been several proposals for the implementation of advanced fuels in LWRs. Relative to traditional fuel (UO_2), they provide heightened safety against accidents, improved cost-effectiveness, enhanced thermal conductivity, and a range of other advantageous features. Research institutes such as NERI (Nuclear Energy Research Institute), MIT (Massachusetts Institute of Technology) and KAERI (Korea Atomic Energy Research Institute) propose modify the conventional fuel geometry changing the cylindrical geometry to the annular geometry, where the main feature is the incorporation of an internal coolant channel into the fuel rods. The primary advantages include reducing the peak temperature within fuel pellet and potentially increasing power generation of reactor, while maintaining safety parameters [1-3]. In addition, different fuel alloys have been studied in order to develop accident-tolerant fuels. The Uranium Mononitride (UN) is a one of candidates due its higher thermal conductivity, higher melting temperature, better fission product retention and higher fissile density compared to conventional UO_2 [4,5]. In this context, the present paper evaluates the use of UO_2 and UN in Annular Fuel Assemblies (AFAs) for a typical PWR. The SCALE

6.0/NEWT and the STHIRP codes are employed to perform neutronic and thermal-hydraulic simulations respectively. Different configurations of AFAs were simulated and compared to Conventional Fuel Assembly (CFA) geometry. This study evaluates different annulus and number of pins for AFAs, but it considers the same fuel enrichment, the same moderator to fuel volume ratio and the same external dimensions for all fuel assemblies. This methodology helps verify the effects of different design parameters on neutronic and thermal-hydraulic parameters. The goal is prospect an advanced fuel assembly for use in a conventional PWR with power of 3.771 MWt.

2. METHODOLOGY

2.1. General description of the used codes

The SCALE 6.0 is a code package developed by ORNL (Oak Ridge National Laboratory) for nuclear reactor physics and radiation shielding analysis. It is indeed used for neutronic studies where the package contains various modules that utilize both stochastic and deterministic methods approaches to solve problems related to neutron transport and radiation shielding. Among the diverse array of modules within SCALE 6.0, one notable component is NEWT that operates as a deterministic code, employing a multi-group discrete ordinates method. Its standout feature lies in its adaptable meshing capabilities, facilitating intricate 2D neutron transport calculations within complex geometries [6].

The STHIRP is a sub-channel thermal hydraulic code developed at the Nuclear Engineering Department of *Universidade Federal de Minas Gerais* (Brazil), which was based in COBRA, VIPRE-01/02 and MATRA-α codes. It encompasses a series of solutions derived from fundamental principles encompassing mass conservation, momentum transfer, and energy balance equations, tailored to the specific conditions of the system under examination. Aiming to verify the reliability of the STHIRP, previous works were developed and the results were very similar to the experimental data [7] and also to results of other sub-channel codes as COBRA-3C and RELAP-5 code [8-10].

2.2. Simulated Models

Five types of Annular Fuel Assemblies were simulated in SCALE/NEWT and STHIRP, encompassing both UO_2 and UN fuel types.

- AFA11 – Annular Fuel Assembly, lattice 11 x 11;
- AFA12 – Annular Fuel Assembly, lattice 12 x 12;
- AFA13 – Annular Fuel Assembly, lattice 13 x 13;
- AFA14 – Annular Fuel Assembly, lattice 14 x 14; and
- AFA15 – Annular Fuel Assembly, lattice 15 x 15.

Aiming to maintaining the pitch distance of the fuel assemblies within the reactor core, the AFAs were structured to match the external dimensions (23 x 23 cm) of a conventional PWR fuel assembly (CFA) with a lattice 16x16, 236 fuel pins and 20 guide thimbles for control rods insertion. The fuel enrichment considers the percentage of advanced fuels (5%) and for the cladding, gap and moderator were used the traditional Zircalloy-4, helium and light water, respectively. Also, to avoid large variations of thermal neutron spectrum, the moderator to fuel volume ratio (V_M/V_F) of the AFAs is the same to CFA. The simulations were carried out without insertion of reactivity control system and burnable absorbers. Fig. 1 depicts the geometry of the simulated fuel assemblies and Tab. 1 presents the main geometrical data of the fuel assemblies.

The SCALE/NEWT model employs the ENDF/B-VII library collapsed into 238 energy groups. It considers the geometry of Fig.1, the data of Tab. 1 and temperatures presented in Tab. 2, which were based in previous studies that describes distinct operational temperatures for different fuel assembly geometry [11].

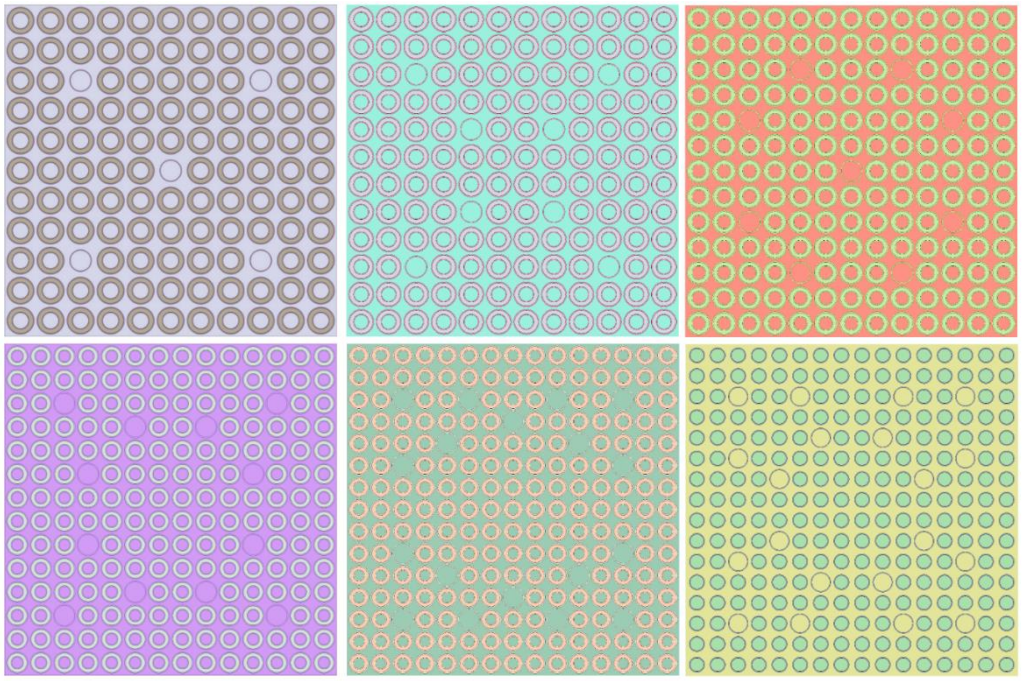

Fig. 1. Annular (AFA11 to AFA15) and Conventional (CFA16) fuel assemblies.

Tab. 1. Geometric data of simulated fuel assemblies

Parameter		**AFA11**	**AFA12**	**AFA13**	**AFA14**	**AFA15**	**CFA16**
Number of Fuel Pins		116	136	160	184	207	236
Number of Guide Tubes		05	08	09	12	18	20
Pitch Distance of Fuel Pins		2.08	1.90	1.76	1.63	1.52	1.43
Moderator Volume, V_M (cm^3)	Inner channel	354.3	279.5	229.2	174.5	139.4	-
	Outer channel	563.2	462.9	402.7	356.2	309.2	444.0
	Total	117123	114707	112059	109294	106428	118066
Fuel Volume, V_F (cm^3)	Total	60248	59005	57643	56220	54746	60733
Ratio V_M/V_F		1.9440	1.9440	1.9440	1.9440	1.9440	1.9440
Fuel assembly dimensions (cm)		23.0 x 23.0					

Tab. 2. Temperature (K) for each fuel pin zone in NEWT model.

Zone	**AFA11**	**AFA12**	**AFA13**	**AFA14**	**AFA15**	**CFA16**
Fuel	973	923	873	848	833	873
Gap	973	923	873	848	833	873
Cladding	753	719	685	667	657	618
Moderator	729	696	664	648	638	587

About the thermal-hydraulic model, in order to decrease the computational time and to reduce the input data of the simulations, the configured geometry in the STHIRP considers a quarter of fuel assemblies' symmetries (Fig. 1). The simulations use as input data the relative power distributions calculated by the SCALE/NEWT to each fuel pin in radial plan. In axial directions the model uses a chopped cosine power distribution.

The Tab. 3 presents the main characteristics of the STHIRP model that were based in traditional references [11,12] and the linear power density (q') that was calculated by the following equation:

$$q' = \frac{P}{L \cdot N \cdot C} \tag{1}$$

where:

- P is the thermal power value used in the simulations;
- L is the active length of the fuel assembly;
- N is the fuel rods number of the configuration; and
- C is the power fraction generated in fuel.

Tab. 3. Main data of thermal-hydraulic model (Nominal Power).

Description		**Unit**	**AFA**					**CFA**
			11	**12**	**13**	**14**	**15**	**16**
Linear power density	UO_2	kW/cm	0.21	0.18	0.15	0.13	0.12	0.10
	UN		0.21	0.18	0.15	0.13	0.12	0.10
Active length of the fuel assembly		m	3.91	3.91	3.91	3.91	3.91	3.91
Initial mass flow (nominal power)	UO_2	kg/s	145	145	145	145	145	92
	UN		220	220	220	220	220	92
Power fraction generated in the fuel		–	0.97	0.97	0.97	0.97	0.97	0.97
Inlet temperature of sub-channels		ºC	291.1	291.1	291.1	291.1	291.1	291.1
Inner diameter of guide tubes		cm	1.400	1.400	1.400	1.400	1.400	1.240
Outer diameter of guide tubes		cm	1.537	1.537	1.537	1.537	1.537	1.380
Inner diameter of fuel pins		cm	1.073	0.953	0.863	0.753	0.673	–
Outer diameter of fuel pins		cm	1.918	1.758	1.623	1.492	1.391	1.077
Pitch distance of fuel pins		cm	2.08	1.90	1.76	1.63	1.52	1.43
Number of fuel rods		–	29	34	40	46	52	59
Number of sub-channels		–	36	49	49	64	64	81
Number of guide tubes		–	1.5	2.0	2.5	3.0	4.5	5.0

In order to evaluate the temperature distribution within the fuel pins, their total volume was subdivided into smaller volumes. Fig. 2 illustrates the employed methodology for the simulated fuel pins. For both models, the axial plan was segmented into 31 parts and the radial plan was sectioned into 11 radial areas. However, they present different subdivisions in radial plan. In radial fuel zone, the conventional solid pin has 8 and the annular pin present 5 parts. In cladding region, solid pin has 3 and annular pin presents 6 (3+3) parts.

For both configurations, the gap composition was not considered, because of the small interference of ^{3}He and ^{4}He in the thermal conductivity compared to the fuel and the cladding. Although the simulated model comprises radial and axial meshes to all fuel rods, the temperature distribution analysis was performed only to the fuel rod with the highest temperature (hottest rod) and to its associate sub-channel. The STHIRP code provides the necessary data for the definition of these two characteristics. This methodology aims to evaluate the most critical pin and the associated coolant.

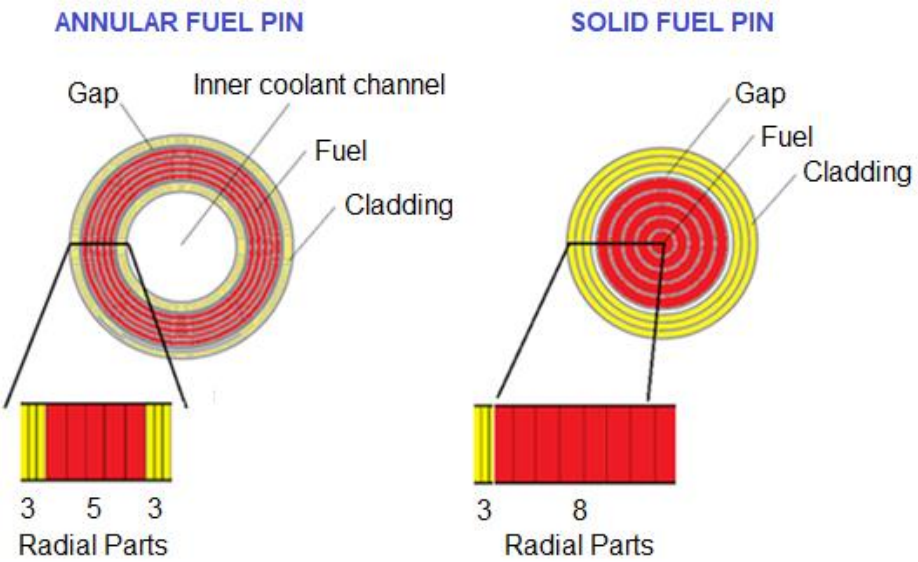

Fig. 2. Radial subdivision in annular and solid fuel pins.

3. RESULTS

3.1. Neutronic Parameters

The Tab.4 presents the infinite multiplication factor (k_{inf}) calculated by SCALE 6.0/NEWT for simulated cases. Between the two fuel types, UN presents the lowest k_{inf} because of the different microscopic cross-sections of the ^{16}O and ^{14}N. In the thermal and epithermal energy ranges, the cross-section values for ^{14}N are higher than ^{16}O, particularly concerning (n, γ) and (n, p) reactions. Despite both fuels having equal enrichment value, this behavior significantly contributes to a notable reduction in the criticality of UN fuel. Regarding the ^{14}N, the cross-section of ^{14}N (n, p)^{14}C is higher than ^{14}N (n, γ)^{15}N. Thus, for this isotope, the (n, p) reaction is the primary cause of reactivity reduction in UN fuel. About the ^{16}O, the (n, γ) reaction has the highest cross section and (n, p) has insignificant influence in the system, because it may occur in the fast region of the spectrum.

Tab. 4. Infinite multiplication factor for evaluated fuel assemblies

Fuel Type	**AFA11**	**AFA12**	**AFA13**	**AFA14**	**AFA15**	**CFA16**
UO_2	1.406725	1.403590	1.402124	1.400361	1.399239	1.432388
UN	1.272303	1.269215	1.268310	1.266870	1.266321	1.296783

In Tab. 4, comparing the different fuel assembly configurations, CFA16 exhibits the highest criticality, while AFA15 demonstrates the lowest, for both UO_2 or UN. The different geometry of simulated models contributes to this behavior. Distinct pin pitch distance, pin dimensions and fuel rods number can significantly influence neutron moderation and absorption within the fuel assembly, affecting k_{inf}. Although all fuel assemblies have the same V_M/V_F, the moderator volume (V_M) and the fuel volume (V_F) are different among the cases (Tab. 1). The results indicate that the k_{inf} is proportional to the volume of the fuel and moderator. The AFA15 has the lowest values of V_M and V_F, and so it presents the lowest k_{inf}. On the other hand, CFA16 has the biggest VM and VF and consequently the highest k_{inf}. The AFA15 has the lowest values of V_M and V_F, resulting in the lowest k_{inf}. Conversely, CFA16 has the largest volumes, leading to the highest criticality. Note that, CFA16 and the AFA11 have similar V_M and V_F and therefore, these configurations present the closest k_{inf} values (Tab. 1).

The Tab. 5 presents the highest and the lowest values of Relative Power Distribution (RPD) in radial plan of the simulated fuel assemblies. In general, RPD are similar among the fuel assemblies and this behavior may be due the same enrichment of ^{235}U in UO_2 and UN. However, the different configuration of fuel assemblies affects the neutron flux and this behavior provokes alterations in RPD values. Among the cases AFA15 exhibits the highest values. Although Tab. 5 presents only the extreme values of RPD, this parameter was calculated for all fuel pins in a CFA and AFAs. These results are essential for the STHIRP simulation, because the RPD values are used in the calculation of thermal hydraulic parameters. In axial directions the STHIRP code uses a chopped cosine power distribution.

Tab. 5. Relative Power Distribution (RPD) for evaluated cases.

RPD	Fuel Type	AFA11	AFA12	AFA13	AFA14	AFA15	CFA16
Highest	UO_2	1.09	1.09	1.07	1.07	1.11	1.06
	UN	1.11	1.10	1.08	1.09	1.12	1.07
Lowest	UO_2	0.95	0.93	0.95	0.95	0.95	0.93
	UN	0.94	0.94	0.94	0.93	0.88	0.92

3.2. Thermal-Hydraulic Parameters

The Tab. 6 and 7 provide the radial temperature distribution (in ºC) of the hottest fuel pin for both conventional and annular geometries. Due to the presence of inner coolant channels, the AFAs exhibit the lowest temperature distribution, as expected. Comparing CFAs and AFAs, the smallest temperature difference at the centerline of the fuel zone is for (UO_2): 1468 – 558 = 910 °C; and for (UN): 668 – 479 = 189 °C. These differences are highest for UO_2 because it exhibits the highest temperature distribution for corresponding geometries. This characteristic is prominent in conventional fuel geometry. The temperature difference between UO_2 and UN for CFAs at the centerline of the fuel region is noticeable (1468 – 668 = 800°C). This behavior is due to the superior thermal conductivity and heat capacity of UN compared to UO_2.

Tab. 6. Radial temperature (ºC) of hottest fuel pins calculated for conventional geometry.

Fuel Type	Fuel Region								Cladding Zone		
	1	2	3	4	5	6	7	8	9	10	11
UO_2	1468	1451	1380	1260	1102	919	728	543	348	325	303
UN	668	665	658	646	628	606	578	546	349	325	303

Tab. 7. Radial temperature (ºC) of hottest fuel pins calculated for annular geometry.

Fuel Type	AFA Type	Cladding Zone			Fuel Region					Cladding Zone		
		1	2	3	4	5	6	7	8	9	10	11
UO_2	11	298	311	324	450	514	558	501	440	324	310	296
	12	299	312	325	451	509	549	497	440	325	310	297
	13	297	309	320	424	466	494	456	414	318	306	295
	14	298	311	322	433	477	505	466	423	321	309	296
	15	299	311	323	434	475	501	464	423	321	308	296
UN	11	298	312	326	457	471	479	467	453	327	311	296
	12	297	311	324	448	460	467	456	444	325	310	296
	13	296	307	318	418	427	432	424	415	318	305	294
	14	297	309	321	430	439	444	436	426	321	308	296
	15	297	310	321	430	439	444	435	426	321	308	296

Regarding to annular configurations, AFA11 exhibits the highest radial temperature distribution, while AFA13 has the smallest one. A set of factors may be generating this behavior because the distinct AFAs configurations induce variations in heated perimeter, wetted perimeter, flow area, power density, among others.

The Tab. 8 presents the Minimal values of Departure from Nucleate Boiling Ratio (MDNBR) for the evaluated cases. Although this table shows only the MDNBR, the STHIRP calculates DNBR for all axial meshes (31 segments) in each fuel pin. Most MDNBR are close to the middle axial plane of the fuel assembly (222 cm) and considering the safety requirement set by regulatory agencies (MDNBR < 1.3), all configurations are within safety limits. The AFA11 and AFA14 have the highest MDNBR for UO_2 and UN, respectively.

Tab.8. MDNBR for nominal reactor power.

Parameter	Fuel Type	AFA11	AFA12	AFA13	AFA14	AFA15	CFA16
MDNBR	UO_2	5.33	5.25	2.27	4.90	3.93	5.84
	UN	9.08	9.34	8.43	9.42	8.74	5.83
Axial Length (cm)	UO_2	222	235	326	248	287	222
	UN	222	235	248	222	235	222

Fig. 3 and 4 illustrate the axial temperature distribution of the hottest coolant channels for UO_2 and UN fuel types. The inlet temperature is equal for all cases (291 ºC), but the outlet temperature exhibits different values, as expected. Although UO_2 and UN have distinct thermal conductivities, the CFAs exhibit similar axial temperature distribution due to the equal temperatures at the last radial section (No. 11) in the cladding zone (Tab. 6). About AFAs, the inner coolant channels (ICC) have higher temperatures than outer coolant channels (OCC) for the same configuration type (Fig. 3 and 4). This behavior can be due to flow area of the sub channels because ICC has smaller values than OCC for all cases (Tab. 9).

Tab. 9. Flow area of coolant channels surrounding the fuel pins.

Flow Area	AFA11	AFA12	AFA13	AFA14	AFA15	CFA16
Inner coolant channels (cm^2)	0.904	0.713	0.585	0.445	0.356	–
Outer coolant channels (cm^2)	1.437	1.183	1.029	0.909	0.791	1.134

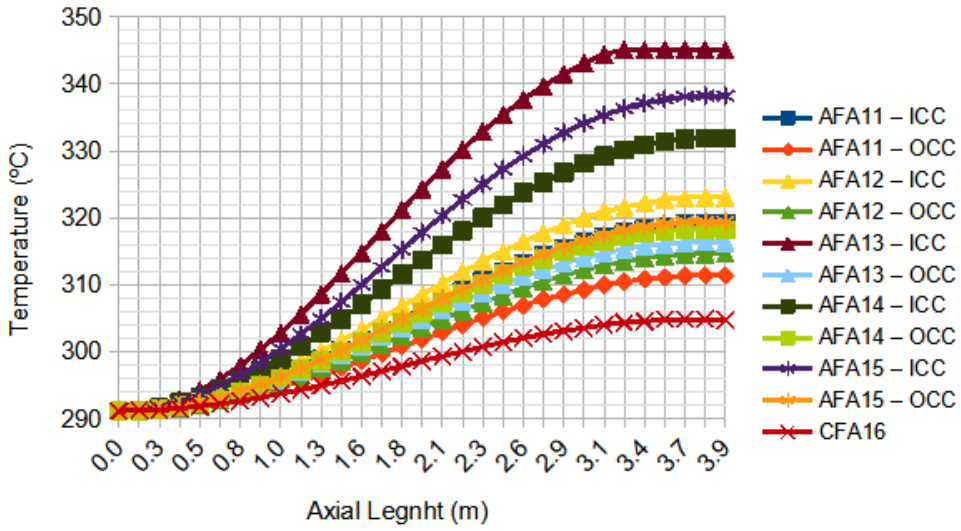

Fig. 3. Axial temperature distribution of the hottest fuel channels of for UO_2 fuel type.

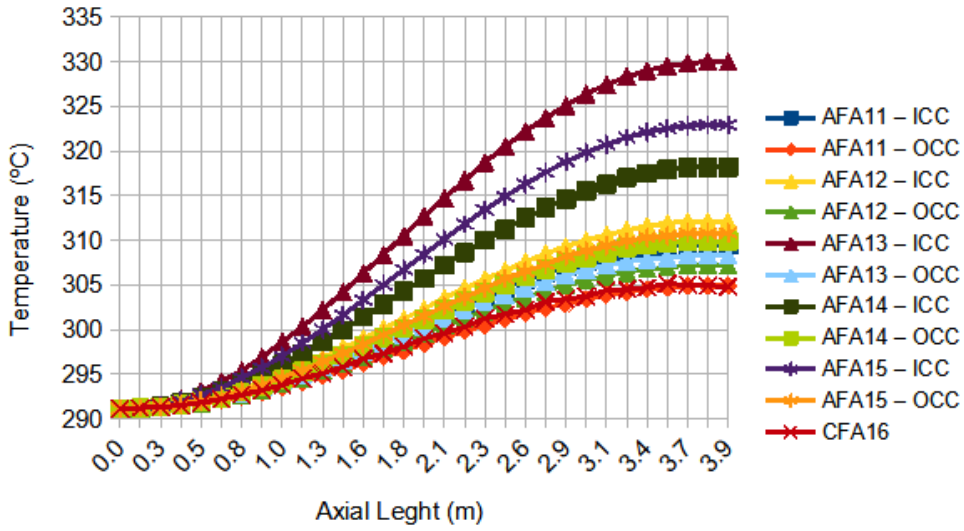

Fig. 4. Axial temperature distribution of the hottest fuel channels of for UN fuel type.

Among annular fuel assemblies, AFA13 demonstrates the highest temperature gradient into ICC. This case has the highest temperature difference between ICC and OCC. This behavior may be due to correlations among several parameters such as linear power density, flow coolant area, DNBR, and others.

Comparing the two fuel types in AFA configurations, UN presents the lowest temperature for the same geometry. This behavior is associated with the smallest fuel pin temperatures of UN in relation to UO_2. For instance, in the case of AFA13, the respective outlet temperatures for ICC and OCC are 330 ºC and 308 ºC with UN, whereas they are 345 ºC and 315 ºC with UO_2. Thus, the temperature difference between ICC and OCC is smaller for UN.

4. CONCLUSIONS

The results confirm some advantageous of UN and annular fuel assemblies compared to conventional geometry UO_2. Both features, the higher thermal conductivity of UN and the presence of internal coolant channels in AFAs, result in a lower fuel temperature when compared to conventional fuel assembly. However, at the coolant-cladding interface, the temperature is similar for same geometry type due to the same thermal conductivity and thickness of the cladding zone (Zircaloy-4). Considering that the nominal power density is limited by peak cladding temperature, the combined use of UN and/or AFAs with other cladding types could contribute to increasing thermal energy generation.

Among annular fuel assemblies, AFA13 has the lowest radial temperature distribution but it presents the highest difference in outlet temperature between inner and outer coolant channels. While all cases remain within safety MDNBR limits, AFA13 exhibits the lowest values, suggesting a more conservative margin. In this context, AFA11 (UO_2) and AFA14 (UN) would be used to evaluate thermal-hydraulic parameters as a function of a power increase due to their highest MDNBR. However, it is important to note that the increase in the reactor power requires, among other factors, an increase in the coolant mass flow in the same order. Thus, the UN and AFAs could be indicated for modular reactors due their better capacity to provide high mass flux than the current power reactors.

ACKNOWLEDGEMENTS

The authors are grateful to the following Brazilian research funding agencies: FAPEMIG (*Fundação de Amparo à Pesquisa do Estado de Minas Gerais*), CAPES (*Coordenação de Aperfeiçoamento de Pessoal de Nível Superior*), CNPq (*Conselho Nacional de Desenvolvimento Científico e Tecnológico*), and CNEN (*Comissão Nacional de Energia Nuclear*). They are thankful to Professor Claubia Pereira of *Universidade Federal de Minas Gerais* (Brazil) for running the simulations in SCALE 6.0.

REFERENCES

[1] A. P. Deokule *et al*., Reactor physics and thermal hydraulic Analysis of annular fuel rod cluster for Advanced Heavy Water Reactor. *Energy Procedia*, Vol. 71, pp. 52-61 (2015).

[2] M. S. Kazimi *et al*., High-Performance Fuel Design for Next Generation PWRs 2nd Annual Report. Massachusetts Institute of Technology. Center for Advanced Nuclear Energy Systems. Nuclear Fuel Cycle Program (2003).

[3] D. Feng *et al*., Innovative fuel designs for high power density pressurized water reactor. Massachusetts Institute of Technology. Center for Advanced Nuclear Energy Systems. Nuclear Fuel Cycle Program (2005).

[4] G. J. Youinou and R. S. Sen, Impact of accident-tolerant fuels and claddings on the overall fuel cycle: a preliminary systems analysis, *Nuclear Technology*, Vol. 188 (2), pp. 123-138 (2014).

[5] E. Speidel, D. Keller, Fabrication and Properties of Hot-Pressed Uranium Mononitride, Technical Report 10.2172/4674236 (1963).

[6] B. T. Rearden and M. A. Jessee, SCALE code system. Oak Ridge National Laboratory (ORNL), Oak Ridge (2018).

[7] M. A. F. Veloso, Análise Termofluidodinâmica de Reatores Nucleares de Pesquisa Refrigerados a Água Em Regime de Convecção Natural, Doctoral Thesis, Faculdade de Engenharia Química, Universidade Estadual de Campinas (UNICAMP), Campinas (2004).

[8] A. R. Hamers *et al*., Analysis of the capability of the COBRA-EN code to reproduce a nine-rod bundle mixing Tests. In: Proceedings of ICAPP 2015, Nice, vol. 1, pp. 1-9 (2015).

[9] P. M. Fortini *et al*., Analysis of mixing tests in a nine-rod bundle. In: International Nuclear Atlantic Conference, INAC 2013, Recife, vol. 1, pp. 1-9 (2013).

[10] A. L. Costa *et al*., Thermal hydraulic analysis of the IPR-R1 TRIGA research reactor using a RELAP5 model, *Nuclear Engineering and Design*, Vol. 240, n. 6, pp. 1487-1494 (2010).

[11] M. S. Kazimi *et al*., High performance fuel design for next generation PWRs: Final report, Massachusetts Institute of Technology. Center for Advanced Nuclear Energy Systems. Nuclear Fuel Cycle Program (2006).

[12] ELETRONUCLEAR, Final Safety Analysis Report - FSAR, Angra 2, Rio de Janeiro (2013).